Journal of Solid State Chemistry **168,** 384–389 (2002)
doi:10.1006/jssc.2002.9685

# Thin Films of Molecular Metals: TTF-TCNQ

J. Fraxedas,*[,1] S. Molas,* A. Figueras,* I. Jiménez,† R. Gago,‡
P. Auban-Senzier,§ and M. Goffman§[,2]

*Institut de Ciència de Materials de Barcelona (CSIC), Campus de la UAB, E-08193 Bellaterra, Spain; †Instituto de Ciencia y Tecnología de Polímeros (CSIC), E-28006 Madrid, Spain; ‡Institut für Ionenstrahlphysik und Materialforschung, Forchungszentrum Rossendorf, Postfach 510119, 01314 Dresden, Germany; and §Laboratoire de Physique des Solides, Bat. 510, Université Paris-Sud, F-91405 Orsay, Cedex, France

Received December 3, 2001; accepted April 23, 2002

**We present recent results on the characterization of highly ordered polycrystalline thin films of the charge transfer salt TTF–TCNQ (TTF = tetrathiafulvalene, TCNQ = tetracyanoquinodimethane) prepared by thermal sublimation in high vacuum under different conditions. The increase in orientation and microcrystal size as a function of substrate and annealing temperatures is addressed. A consequence of such an increase is the reduction of the conductivity activation energy, which eventually leads to the observation of the Peierls transition by resistivity measurements. X-ray absorption near edge spectroscopy studies performed with synchrotron radiation reveal directly the influence of charge transfer on unoccupied states near the Fermi level.** 

***Key Words:*** **molecular metals; molecular organic materials; thin films; TTF-TCNQ; Peierls transition; synchrotron radiation.**

## INTRODUCTION

The interest in the preparation of thin films of molecular organic materials stems from their potential applications in microelectronics, nanotechnology, biotechnology, nonlinear optics, light-emitting devices, field effect transistors, liquid crystals, etc. (1) and from their multifunctional character (2). The recent discovery of ambipolarity, coherent light emission and superconductivity in neutral molecular organic materials upon charge injection (3) has increased the effort in the preparation of highly pure, crystalline and oriented thin films. Such films can be obtained by organic chemical vapor deposition (OCVD) (4), thermal sublimation in vacuum (5), organic vapor-phase deposition (OVPD) (6), organic molecular beam deposition (OMBD) (7), co-evaporation (8), the Langmuir–Blodgett technique (9) and electrochemical crystallization (10). Recently, the preparation of thin single crystals by confined electrocrystallization has been reported (11).

In the present work, we will basically focus on the well-known molecular metal TTF–TCNQ (TTF = tetrathiafulvalene, TCNQ = tetracyanoquinodimethane) as a case study because its physical properties have been extensively studied in single crystals and because it exhibits a single crystallographic phase and stable surfaces. TTF–TCNQ ($P2_1/c$, $a = 1.2298$ nm, $b = 0.3819$ nm, $c = 1.8468$ nm, $\beta = 104.46^\circ$) is a charge transfer salt (bulk partial charge transfer $\rho = 0.59$) exhibiting monoclinic crystal structure built up from parallel, segregated chains of donors (TTF) and acceptors (TCNQ) (12). Its 1D metallic behavior arises from the $\pi$-overlap along the stack ($b$-axis). The electrical conductivity is highly anisotropic: $\sigma_b/\sigma_a \sim 10^3$ at room temperature, where $\sigma_a$ and $\sigma_b$ represent the conductivity along the $a$- and $b$-directions, respectively. A charge density wave with wave vector $2k_F$, where $k_F$ stands for the Fermi wave vector, develops below 54 K on the TCNQ chains and eventually brings the system into an insulating ordered state below 38 K (13).

Thin TTF–TCNQ films grown by CVD (4, 14) and by thermal sublimation in vacuum (5, 15) are described in the literature. Thin films of the superconducting phase $\alpha_t$-(BEDT-TTF)$_2$I$_3$ (BEDT-TTF = bis(ethylenedithio-tetrathiafulvalene)) have been also obtained by evaporation in vacuum (16) and conductive films of BEDT-TTF doped with $ClO_4^-$ anions have been prepared by a combination of vacuum deposition of the donor molecules on gold electrodes with an electrochemical process (17). Highly conductive thin films of $(TTF)_7I_5$ have been also reported by double source evaporation (18).

The thin TTF–TCNQ films are astonishingly stable even when stored in air for several months as confirmed by atomic force microscope (AFM) measurements (19). Their stoichiometric desorption in ultra-high vacuum (UHV) has

[1] To whom correspondence should be addressed. Fax: +-34-9-3-580-5729. E-mail: fraxedas@icmab.es.
[2] Present address: DRECAM/SCM,CEA Saclay, F-91191 Gif sur Yvette Cedex, France.



0022-4596/02 $35.00

permitted the determination of the valence band dispersion close to the Fermi level with angle-resolved ultraviolet photoemission spectroscopy (ARUPS) (20), which is nearly identical to that obtained with in situ cleaved single crystals (21). The preparation of stable, highly oriented thin films of metallic organic materials offers thus the possibility to obtain available areas for ARUPS studies larger than those typically at hand with single crystals. This appears therefore as a promising alternative to the growth of single crystal samples for the experimental determination of their electronic structure (band mapping). Finally, the nanomechanical properties of thin films of TTF–TCNQ have been recently determined with AFM, exhibiting Young's modulus of ca. 20 GPa (22).

## EXPERIMENTAL SECTION

Thin films (thickness $\sim 1\,\mu m$) have been obtained by thermal sublimation in high vacuum ($\sim 10^{-6}$ mbar) of recrystallized TTF–TCNQ powder. *Ex situ* cleaved alkali halide substrates (NaCl(001), KCl(001) and KBr(001)) as well as sputter-deposited $Si_3N_4$ films were used as substrates. The evaporation temperature was $\approx 430$ K with substrate temperatures $T_s \leq 325$ K and the samples were in situ annealed at temperatures $T_a \leq 360$ K in nitrogen (nitrogen pressure slightly above ambient pressure). The preferential orientation of the films has been studied by X-ray diffraction (XRD) using a Philips Material Research Diffractometer system with a four circle goniometer and parallel beam optics. The scanning electron microscope (SEM) images were obtained with a Hitachi S-570 equipment.

Information on the density of unoccupied electronic states was obtained by X-ray absorption near edge spectroscopy (XANES). This technique is based on the induction of intraatomic interband transitions from core levels to empty states caused by incident X-rays of sufficient energy. Therefore, the partial (element selective) density of unoccupied states is obtained (23). The XANES measurements were performed at the SACEMOR endstation (beamline SA72) of the *Laboratoire pour l' Utilisation du Rayonnement Electromagnetique* (LURE) in Orsay, France and at the beamline 8.2 of the Stanford Synchrotron Radiation Laboratory (SSRL) in Stanford, CA, USA. The data were acquired in the total electron yield mode by measuring with an ammeter the current drain to the ground. The signal was normalized to the simultaneously recorded photocurrent from a gold-covered grid.

Resistivity ($\rho$) measurements were performed using the four contacts low frequency lock-in technique with a measuring current of 10 and 0.1 μA (see details below). Gold wires with a diameter of 17 μm were previously attached with silver paint to four parallel gold stripes evaporated on the films.

## RESULTS AND DISCUSSION

### *XRD and SEM*

Figure 1a shows the XRD pattern of a thin TTF–TCNQ film grown on an *ex situ* cleaved KCl(100) substrate. Only (00*l*) reflections are observed for even values of *l*, indicating that the films are oriented with their (002) molecular planes (*ab*-planes) parallel to the substrate surface. The films consist of highly oriented and strongly textured rectangular-shaped microcrystals, with their *a*- and *b*-axis parallel to both [110] and [$\bar{1}$10] substrate directions, respectively, due to the cubic symmetry of the substrate (not shown) (24).

Figure 1b shows the rocking curves of the (002) reflection of films obtained under different experimental conditions: (#1) $T_s = 300$ K and $T_a = 350$ K, (#2) $T_s = 310$ K and $T_a = 360$ K and (#3) $T_s = 325$ K and $T_a = 350$ K. We observe a clear decrease of the full-width at half-maximum (FWHM) of the rocking curves from 1.0° to 0.5° upon

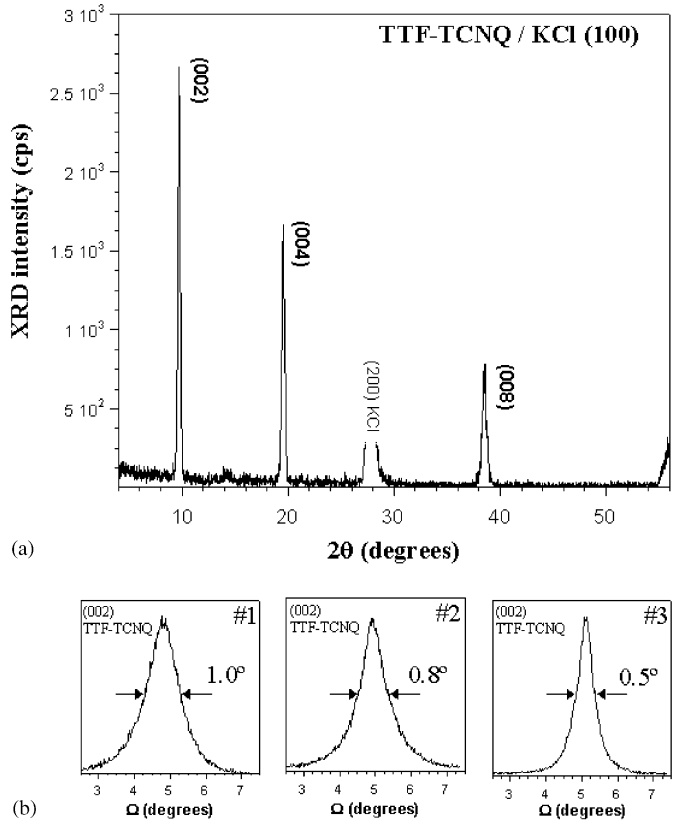


**FIG. 1.** (a) XRD pattern ($\theta$-2$\theta$) of TTF–TCNQ/KCl(100). (b) Rocking curves of the (002) reflection of films obtained under different experimental conditions: (#1) $T_s = 300$ K and $T_a = 350$ K, (#2) $T_s = 310$ K and $T_a = 360$ K and (#3) $T_s = 325$ K and $T_a = 350$ K.

increase of the substrate temperature from 300 to 325 K, for a similar annealing temperature, evidencing an increase of the (002) plane orientation. When the films are grown at $T_s = 300$ K without annealing, FWHM $\approx 1^\circ$. The films become thus highly oriented already when the substrates are held at room temperature but significantly increase their degree of orientation by a moderate increase of temperature (in this case 25 K). This is associated to the weak (van der Waals and hydrogen bonding) intermolecular and molecule–substrate interactions. In general, highly crystalline and ordered thin films of TTF-derivatives on alkali halide substrates at moderate substrate temperatures (below 325 K) are obtained due to the weak interactions involved in the formation of the films (25). When the materials exhibit polymorphism, a temperature increase may activate a phase transition (i.e., the $\alpha$-phase of (BEDT-TTF)$_2$I$_3$ transforms to the superconducting $\alpha_t$-phase upon annealing at ca. 360 K (16)), or a change of stoichiometry (i.e., by confined electrocrystallization superconducting $\kappa$-(BEDT-TTF)$_2$Cu(NCS)$_2$ is selectively grown at 300 K, while the insulating phase, (BEDT-TTF)Cu$_2$(NCS)$_3$, is obtained instead at 335 K (11)).

Figure 2 shows SEM images of films #1, #2 and #3 (KCl(100) substrates) and also #4, obtained on amorphous $Si_3N_4$ substrates ($T_s = 310$ K and $T_a = 360$ K). Films #1, #2 and #3 exhibit an increase of the microcrystals size upon increasing the substrate temperature. When the films are grown at $T_s = 300$ K and $T_a = 350$ K (#1) the mean length of the microcrystals along the long axis (*b*-axis) is ca. 1.4 μm, increasing to ca. 2.7 μm when $T_s = 310$ K and $T_a = 360$ K (#2) and up to about 4.9 μm when obtained at $T_s = 325$ K and $T_a = 350$ K (#3). When the KCl(100) substrates are held at room temperature, we observe that the microcrystals are equally distributed in perpendicular directions. In addition to the increase in size with increasing substrate temperature, the microcrystals in the same direction tend to agglomerate leaving, however, the final microcrystal distribution unaltered (no temperature-induced in-plane preferential orientation). In the case of sample #3, a considerable number of microcrystals become curved. This is due to the triggering of in-plane growth directions other than the equivalent [110] caused by the different temperature-induced contributions of the electrostatic and van der Waals interactions to the total energy at the interface (26). Film #4 shows a random distribution of microcrystals (mean length along the *b*-axis $\sim 3.2$ μm) due to the amorphous character of the substrate.

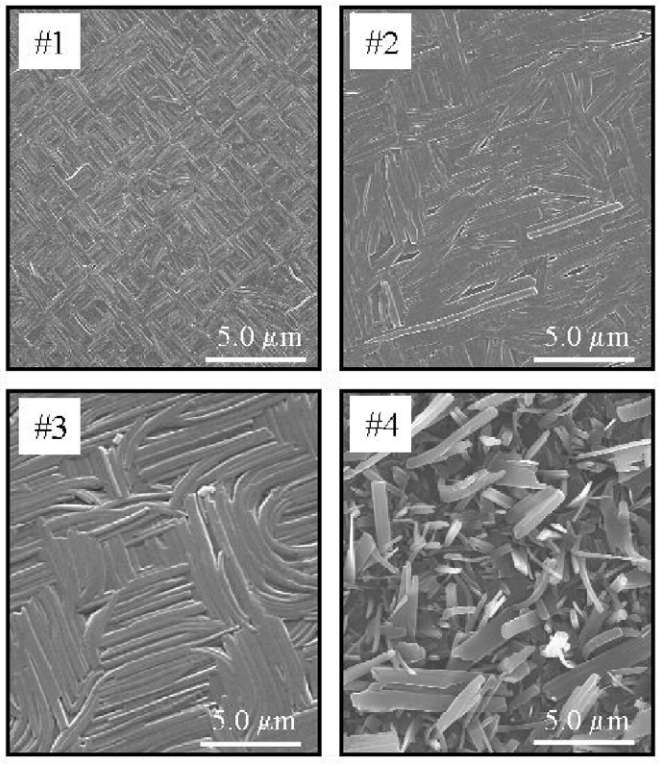


**FIG. 2.** SEM images of TTF–TCNQ/KCl(100) films obtained at: (#1) $T_s = 300$ K and $T_a = 350$ K, (#2) $T_s = 310$ K and $T_a = 360$ K and (#3) $T_s = 325$ K and $T_a = 350$ K and of TTF–TCNQ/$Si_3N_4$ films (#4) obtained at $T_s = 310$ K and $T_a = 360$ K.

## *XANES Measurements*

In the case of charge transfer compounds, it is interesting to determine the modification of the electronic structure of the molecules as a result of the formation of the compound. In particular, we have characterized by XANES the density of unoccupied states comparing the salt with neutral TTF and TCNQ in order to readily verify differences in electronic structure.

Figure 3 shows the XANES spectra associated to relevant core levels: (left) S(2*p*), (center) C(1*s*) and (right) N(1*s*). For each core level the top and center-bottom curves correspond to the TTF–TCNQ (thin films grown at $T_s = 300$ K with no annealing) and to neutral TTF and TCNQ (powder), respectively. Microcrystalline powders of TTF and TCNQ were suspended in ethanol by stirring, and deposited on a silicon wafer immersed in the suspension. The XANES spectra of TTF–TCNQ powder (used for film preparation) are similar to those of TTF–TCNQ thin films but exhibiting traces of contamination (not shown). TTF–TCNQ is thus purified during sublimation as expected. Note the absence of N(1*s*) signal from the TTF powder (right) and absence of S(2*p*) from TCNQ (left), as expected from their atomic composition, thus confirming the purity of the substances. All spectra show a low-energy region, composed of multiple peaks, which corresponds to transition to $\pi^*$ states, followed by a featureless threshold at higher energies associated to the onset of transitions to $\sigma^*$ states. The sharp $\pi^*$ peaks have excitonic origin (27).

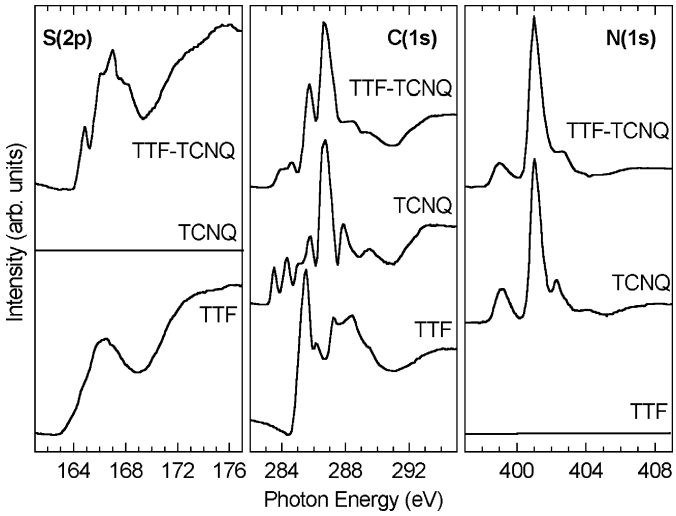


**FIG. 3.** S(2*p*), C(1*s*) and N(1*s*) XANES spectra from thin films ($T_s = 300$ K, no annealing) of the charge transfer compound TTF–TCNQ and from neutral TTF and TCNQ.

A closer observation of the S(2*p*) spectra (left of Fig. 3) reveals that the spectral lineshape is broader for the neutral TTF molecule than for TTF–TCNQ. The opposite trend is observed for the C(1*s*) and N(1*s*) spectra in TCNQ, which are narrower in the neutral state as compared to the TTF–TCNQ salt. The explanation stems from the charge transferred upon the formation of the TTF–TCNQ compound from the donor TTF to the acceptor TCNQ. The extra charge that is accommodated in the compound within the TCNQ electronic structure broadens its electronic levels, whereas the loss of charge in TTF narrows the lineshape of the corresponding states. This is thus a rather direct method to experimentally determine the influence of charge transfer on the unoccupied electronic states close to the Fermi level.

Further details are observed by comparing the C(1*s*) spectra from TTF–TCNQ with the sum of the C(1*s*) signals from neutral TTF and TCNQ, as is shown in Fig. 4. The spectrum from the charge transfer compound largely resembles the sum of the spectra from the neutral molecules. However, some subtle changes are observed, affecting the states derived from the acceptor molecule TCNQ: (i) the two low-energy peaks at 283.5 and 284.3 eV in the sum spectrum appear broader in TTF–TCNQ and shifted $\sim 0.35$ eV towards higher energies, (ii) the peak at 287.9 in the sum spectrum, due to TCNQ states is almost absent in the spectrum from the compound. The states derived from the TTF molecule remain, however, largely unaffected. In order to ascertain the origin of the peaks in the spectra and of their changes elaborated theoretical calculations of the band structure of TTF, TCNQ and TTF–TCNQ should be performed, which, to our knowledge, are not available.

*Resistivity Measurements*

Figure 5a shows resistivity measurements as a function of temperature performed on films grown at: $T_s = 300$ K and $T_a = 350$ K (#1a and #1b) and $T_s = 325$ K and $T_a = 350$ K (#3). The measuring currents were 10 μA for #1a and 0.1 μA for #1b and #3. The conduction barrier energy or activation energy Δ can be obtained from the expression $\rho = \rho_0 \exp(\Delta/2k_B T)$, where $k_B$ stands for the Boltzmann constant. From the Arrhenius plot we derive: $\Delta/k_B = 296.8$ and 295.4 K for the nominally identical samples #1a and #1b, respectively (grown in different experiments) and 273.7 K for sample #3. Earlier reported values of Δ for oriented thin TTF–TCNQ films lie within 174.0 and 580.0 K (14, 28). The decrease of the conduction barrier energy upon the increase of the substrate temperature is in line with the increase of the microcrystal shape, which reduces the number of grain boundaries. At room temperature, the measured electrical conductivities are: $\sigma = 5.0\,\mathrm{S\,cm^{-1}}$ (#1a), $\sigma = 9.1\,\mathrm{S\,cm^{-1}}$ (#1b) and $\sigma = 2.2\,\mathrm{S\,cm^{-1}}$ (#3), to be compared with earlier determinations on thin films ($5 < \sigma < 30\,\mathrm{S\,cm^{-1}}$) (4, 14, 28, 29), the conductivity of the films resulting from a random contribution of $\sigma_a$ and $\sigma_b$ values. For single crystals $\sigma_b \sim 500\,\mathrm{S\,cm^{-1}}$ at room temperature (30). The fact that sample #3 shows the lowest conductivity value ($2.2\,\mathrm{S\,cm^{-1}}$) in spite of exhibiting a higher degree of orientation, lower activation energy and larger microcrystals is ascribed to insufficient statistics.

A detail of the resistivity vs temperature is displayed for the 273.7 K conduction energy barrier sample #3 in Fig. 5b. The non-linear increase of resistivity below ca. 50 K corresponds to the well-known metal–insulator transition (Peierls transition) accurately determined in single crystals

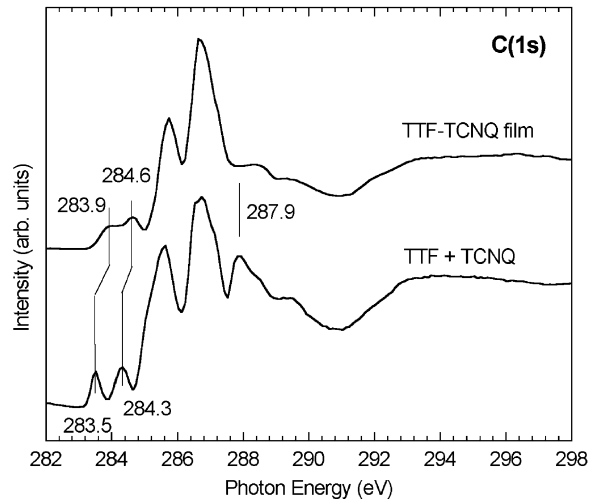


**FIG. 4.** C(1s) XANES spectrum from thin TTF–TCNQ films compared with the sum of the spectra of neutral TTF and TCNQ.

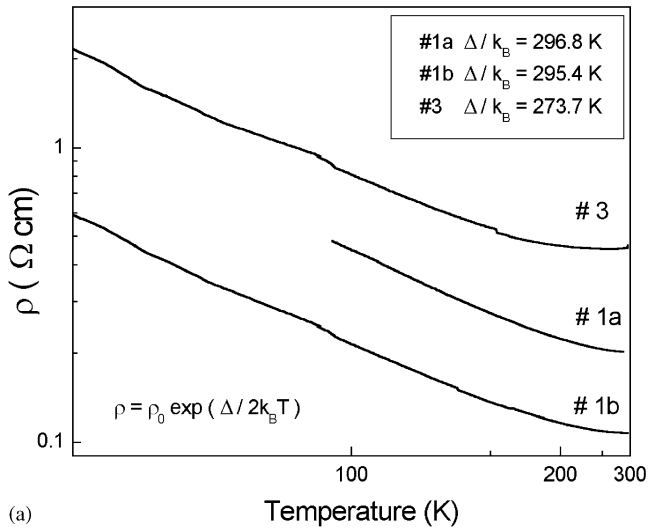


(a)

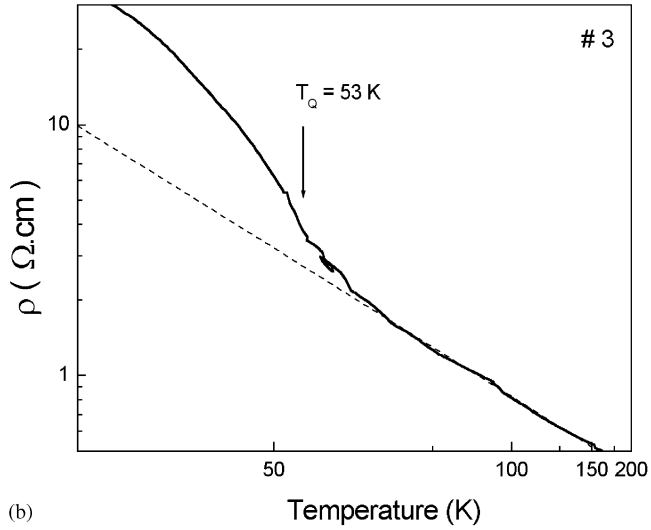


(b)

**FIG. 5.** (a) Resistivity measurements as a function of temperature on thin TTF–TCNQ films grown at: (#1a and #1b) Ts = 300 K and Ta = 350 K and (#3) Ts = 325 K and Ta = 350 K, (b) Detail of the resistivity vs temperature for the sample #3 showing the Peierls transition. The dashed line corresponds to a linear interpolation of the higher temperature region.

(30) and also previously observed on thin films grown by CVD (4). The Peierls transition is more readily observed on the $\Delta/k_B = 273.7$ K sample because of its lower activation energy as compared to the ca. $\Delta/k_B = 296$ K samples.

## OUTLOOK

The preparation of high-quality thin films of not only molecular metals but also of semiconducting and magnetic materials is evidencing an increasing activity because of the appealing applications of such materials in different fields. If large areas of highly crystalline materials are requested the present growth techniques should be improved, specially when thinking of superconducting materials, and different new approaches should be investigated (i.e., the use of chemically modified surfaces as substrates, multi-stage or sequential growth, etc.) When modifying the growth conditions new crystallographic phases are to be expected with perhaps unexpected properties.

## ACKNOWLEDGMENTS

We thank J. Santiso for helping us in the XRD measurements and for fruitful discussions. We thank Ministerio de Ciencia y Tecnología (Spain, project MAT1999-1128) for Financial support.

## REFERENCES

1. C. Bosshard, K. Sutter, P. Prêtre, J. Hulliger, M. Flörsheimer, P. Kaatz, and P. Günter, "Organic Nonlinear Optical Materials." Gordon & Breach, Amsterdam, 1995; A. Ulman, *Chem. Rev.* **96,** 1533 (1996); C.-M. Chan, T.-M. Ko, and H. Hiraoka, *Surf. Sci. Rep.* **24,** 1 (1996); P. Calvert and P. Rieke, *Chem. Mater.* **8,** 1715 (1996); N. A. Peppas and J. J. Sahlin, *Biomaterials* **17,** 1553 (1996); S. R. Forrest, *Chem. Rev.* **97,** 1793 (1997); F. Hide, M. A. Díaz-García, B. J. Schwartz, and A. J. Heeger, *Acc. Chem. Res.* **30,** 430 (1997); P. F. Van Hutten, V. V. Krasnikov, and G. Hadziioannou, *Acc. Chem. Res.* **32,** 257 (1999); Y. Shirota, *J. Mater. Chem.* **10,** 1 (2000); B. Crone, A. Dodabalapur, Y.-Y. Lin, R. W. Filas, Z. Bao, A. LaDuca, R. Sarpeshkar, H. E. Katz, and W. Li, *Nature* **403,** 521 (2000); W. Brütting, S. Berleb and A. G. Mückl, *Org. Electron.* **2,** 1 (2001); J.-C. P. Gabriel, F. Camerel, B. J. Lemaire, H. Desvaux, P. Davidson, and P. Batail, *Nature* **413,** 504 (2001).
2. E. Coronado, J. R. Galán-Mascarós, C. J. Gómez-García, and V. Laukhin, *Nature* **408,** 447 (2000).
3. J. H. Schön, S. Berg, Ch. Kloc, and B. Batlogg, *Science* **287,** 1022 (2000); J. H. Schön, A. Dodabalapur, Ch. Kloc, and B. Batlogg, *Science* **290,** 963 (2000); J. H. Schön, Ch. Kloc, and B. Batlogg, *Nature* **406,** 702 (2000); J. H. Schön, Ch. Kloc, R. C. Haddon, and B. Batlogg, *Science* **288,** 656 (2000).
4. A. Figueras, J. Caro, J. Fraxedas, and V. Laukhin, *Synth. Met.* **102,** 1607 (1999).
5. P. Chandhari, B. Scott, R. Laibowitz, Y. Tomkiewich, and J. Torrance, *Appl. Phys. Lett.* **24,** 439 (1974); T. H. Chen, and B. H. Schetchman, *Thin Solid Films* **30,** 173 (1975); W. Vollmann, W. Berger, C. Hamann, and L. Libera, *Thin Solid Films* **111,** 7 (1984); J. Fraxedas, J. Caro, A. Figueras, P. Gorostiza, and F. Sanz, *J. Vac. Sci. Technol. A* **16,** 2517 (1998).
6. M. Baldo, M. Deutsch, P. Burrows, H. Gossenberger, M. Gerstenberg, V. Ban, and S. Forrest, *Adv. Mater.* **10,** 1505 (1998).
7. A. Koma, *Prog. Crystal Growth Charact.* **30,** 129 (1995); A. Borghesi, A. Sassella, R. Tubino, S. Destri, and W. Porzio, *Adv. Mater.* **10,** 931 (1998); S. Prato, L. Floreano, D. Cvetko, V. DeRenzi, A. Morgante, S. Modesti, F. Biscarini, R. Zamboni, and C. Taliani, *J. Phys. Chem. B* **103,** 7788 (1999).
8. M. Yudasaka, K. Hironaga, H. Yamochi, and G. Saito, *J. Appl. Phys.* **70,** 3501 (1991).
9. H.-S. Wang and Y. Ozaki, *Langmuir* **16,** 7070 (2000).
10. A. C. Hillier, J. H. Schott, and M. D. Ward, *Adv. Mater.* **7,** 409 (1995).

11. A. Deluzet, S. Perruchas, H. Bengel, P. Batail, S. Molas, and J. Fraxedas, *Adv. Funct. Mater.* **12,** 123 (2002).
12. T. J. Kistenmacher, T. E. Philips, and D. O. Lowan, *Acta Crystallogr. B* **30,** 763 (1974).
13. T. Ishiguro, K. Yamaji, and G. Saito, "Organic Superconductors," 2nd ed, p.15. Springer, Berlin, 1998.
14. D. de Caro, J. Sakah, M. Basso-Bert, C. Faulmann, J.-P. Legros, T. Ondarçuhu, C. Joachim, L. Ariés, L. Valade, and P. Cassoux, *C. R. Acad. Sci. Paris Chemistry* **3,** 675 (2000).
15. K. Yase, N. Ara, and A. Kawazu, *Mol. Cryst. Liq. Cryst.* **247,** 185 (1994).
16. K. Kawabata, K. Tanaka, and M. Mizutani, *Adv. Mater.* **3,** 157 (1991); M. Kilitziraki, J. Moldenhauer, H. Wachtel, D. Schweitzer, B. Gompf, W. Eisenmenger, P. Bele, H. Brunner, and H. J. Keller, *Synth. Met.* **70,** 791 (1995); A. J. Moore and M. R. Bryce, *Thin Solid Films* **335,** 209 (1998).
17. Y. F. Miura, S. Ohnishi, M. Hara, H. Sasabe, and W. Knoll, *Appl. Phys. Lett.* **68,** 2447 (1996).
18. M. Yudasaka, K. Hironaga, H. Yamochi, and G. Saito, *J. Appl. Phys.* **70,** 3501 (1991).
19. J. Fraxedas, J. Caro, A. Figueras, P. Gorostiza, and F. Sanz, *Surf. Sci.* **395,** 205 (1998)
20. C. Rojas, J. Caro, M. Grioni, and J. Fraxedas, *Surf. Sci.* **482–485,** 546 (2001).
21. F. Zwick, D. Jérome, G. Margaritondo, M. Onellion, J. Voit, and M. Grioni, *Phys. Rev. Lett.* **81,** 2974 (1998).
22. J. Caro, J. Fraxedas, P. Gorostiza, and F. Sanz, *J. Vac. Sci. Technol. A* **19,** 1825 (2001).
23. A. Curioni, W. Andreoni, R. Treusch, F. J. Himpsel, E. Haskal, P. Seidler, C. Heske, S. Kakar, T. Van Buuren, and L. J. Terminello, *Appl. Phys. Lett.* **72,** 1575 (1998).
24. J. Caro, J. Fraxedas, J. Santiso, A. Figueras, P. Gorostiza, and F. Sanz, *Synth. Met.* **102,** 1607 (1999).
25. S. Molas, J. Caro, J. Santiso, A. Figueras, J. Fraxedas, C. Mézière, M. Fourmigué, and P. Batail, *J. Cryst. Growth* **218,** 399 (2000).
26. J. Caro, J. Fraxedas, and A. Figueras, *Chem. Vapour Deposition* **3,** 263 (1997).
27. P. E. Batson, *Phys. Rev. B* **48,** 2608 (1993); Y. Ma, P. Skytt, N. Wassdahl, P. Glans, D. C. Mancini, J. Guo, and J. Nordgren, *Phys. Rev. Lett.* **71,** 3725 (1993).
28. C. Reinhardt, W. Vollmann, C. Harmann, L. Libera, and S. Trompler, *Krist. Tech.* **13,** 243 (1980) and references therein.
29. T. Sumimoto, K. Kudo, T. Nagashima, S. Kuniyoshi, and K. Tanaka, *Synth. Met.* **70,** 1251 (1995).
30. E. M. Conwell (Ed.), "Semiconductors and Semimetals, Highly Conductive Quasi-One Dimensional Organic Crystals," Vol. 27. Academic Press, London, 1998.